

# Kinetics of desolvation from crystalline inclusion compounds of a diol host with methanol and ethanol

2 PERKIN

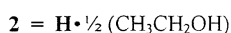
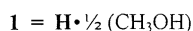
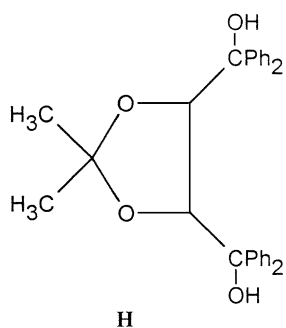
Susan A. Bourne,<sup>\*,a</sup> Bruce M. Oom<sup>a</sup> and Fumio Toda<sup>b</sup>

<sup>a</sup> Chemistry Department, University of Cape Town, Rondebosch 7700, South Africa

<sup>b</sup> Department of Industrial Chemistry, Faculty of Engineering, Ehime University, Matsuyama 790, Japan

The crystal structures of the inclusion compounds of (4*R*,5*R*)-4,5-bis(hydroxydiphenylmethyl)-2,2-dimethyl-1,3-dioxolane with methanol and ethanol have been elucidated. Their isothermal kinetics of desolvation have been studied. Both lose the guest in a single deceleratory step, and a kinetic model based on a diffusion mechanism was found to be the best description for this process.

An investigation of the kinetic parameters associated with the formation and destruction of inclusion compounds is expected to be of great value in determining the viability of a host compound as a means of separating closely related compounds. The kinetics of desorption of inclusion compounds have not been extensively studied, but recently those of two *trans*-9,10-dihydroxy-9,10-dihydroanthracene derivatives with benzene were reported.<sup>1</sup> The kinetics of desolvation of 2,2'-bis(2,7-dichloro-9-hydroxy-9-fluorenyl)biphenyl with 1,4-dioxane and 1,3-dioxolane have also been studied<sup>2</sup> and a method was described for the kinetic analysis of a two step desolvation reaction. For the related host, 2,2'-bis(9-hydroxy-9-fluorenyl)biphenyl, its structure with diethyl ether was elucidated, and the vapour pressure of this clathrate was measured as a function of temperature, yielding an accurate value of the enthalpy change for the desolvation, as well as the activation energy of the reaction.<sup>3</sup> Recently, it has been demonstrated that such desolvation reactions can be monitored by a combination of both thermogravimetry and X-ray diffraction over a wide temperature range, yielding a consistent mechanism for the reaction and a linear Arrhenius plot.<sup>4</sup> We have therefore undertaken the study of the kinetics of desorption of methanol and ethanol from their inclusion compounds with (4*R*,5*R*)-4,5-bis(hydroxydiphenylmethyl)-2,2-dimethyl-1,3-dioxolane, **H**.



**H** has previously been shown to include both primary and secondary amines.<sup>5</sup>

## Experimental

### Crystal growth and data collection

Inclusion compounds were prepared by dissolving the host in an excess of dried alcohol. Crystals were obtained by slow

evaporation of the solutions. X-Ray diffraction data were measured on an Enraf-Nonius CAD4 diffractometer using graphite monochromated Mo-K $\alpha$  radiation ( $\lambda = 0.7107 \text{ \AA}$ ) and the  $\omega$ - $2\theta$  scan mode. During data collection, three reference reflections were monitored periodically to check crystal stability and orientation. The data reduction included correction for Lorentz-polarisation effects. Crystal data and structural parameters are given in Table 1.

### Structure solution and refinement

The structures of the methanol (**1**) and ethanol (**2**) inclusion compounds of **H** were solved by direct methods using SHELXS-86<sup>6</sup> and refined by least-squares methods on  $F^2$  using SHELXL93.<sup>7</sup> Direct methods yielded all the non-hydrogen atoms of the host molecules. The alcohol guests were located in subsequent difference electron density maps. Despite repeating the data collection of **1** at 100 K, many reflections were weak. For this reason, only the oxygens and the carbons in the central ring of **H** were refined anisotropically. All non-hydrogen atoms in **2** were refined anisotropically. The hydroxy hydrogen atoms were not located in difference electron density maps and were therefore omitted from the final model. All other hydrogens were placed with geometric constraints and refined with a common isotropic temperature factor. Further details of the refinement are given in Table 1.

### Thermal analysis

Differential scanning calorimetry (DSC) and thermogravimetry (TG) were performed on a Perkin-Elmer PC7 series system. Finely powdered specimens were placed in open platinum pans for TG and in crimped, but vented aluminium pans for DSC experiments. The sample mass in each case was 3–5 mg. The temperature range was 30–220 °C at a heating rate of 20 °C min<sup>-1</sup>. The purge gas was dry nitrogen flowing at *ca.* 40 cm<sup>3</sup> min<sup>-1</sup>. Data for the kinetics of desolvation were obtained from isothermal TG experiments carried out at selected temperatures in the range 100–130 °C.

## Results and discussion

### Crystal and molecular structure

The inclusion compounds **1** and **2** are isostructural, crystallizing in  $P2_12_12_1$ , with almost identical packing motifs.† The

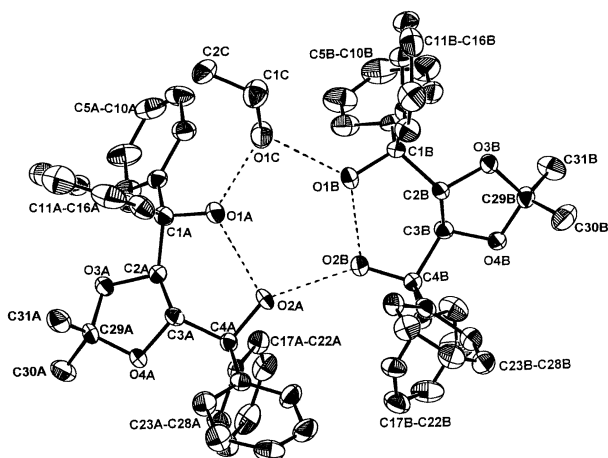
† Atomic coordinates, bond lengths and angles within expected ranges,<sup>8</sup> and thermal parameters have been deposited at the Cambridge Crystallographic Data Centre (CCDC). For details of the deposition scheme, see 'Instructions for Authors', *J. Chem. Soc., Perkin Trans. 2*, 1997, Issue 1. Any request to the CCDC for this material should quote the full literature citation and the reference number 188/52.

**Table 1** Crystal data and details of structure refinement

Compound	1	2
Empirical formula	C <sub>63</sub> H <sub>64</sub> O <sub>9</sub>	C <sub>64</sub> H <sub>66</sub> O <sub>9</sub>
Formula mass	965.14	979.17
<i>T</i> /K	100	294
Crystal system	Orthorhombic	Orthorhombic
Space group	<i>P</i> 2 <sub>1</sub> 2 <sub>1</sub> 2 <sub>1</sub>	<i>P</i> 2 <sub>1</sub> 2 <sub>1</sub> 2 <sub>1</sub>
<i>a</i> /Å	9.051(4)	9.244(5)
<i>b</i> /Å	20.031(6)	20.184(5)
<i>c</i> /Å	28.49(1)	28.684(7)
<i>V</i> /Å <sup>3</sup>	5164(3)	5352(3)
<i>Z</i>	4	4
<i>D</i> <sub>c</sub> /g cm <sup>-3</sup>	1.241	1.215
<i>μ</i> /mm <sup>-1</sup>	0.08	0.08
<i>F</i> (000)	2056	2008
Crystal size/mm	0.25 × 0.28 × 0.28	0.25 × 0.25 × 0.30
<i>θ</i> range/°	1–25	1–25
Index ranges, <i>h</i> , <i>k</i> , <i>l</i>	10, 23, 33	11, 24, 34
Reflections collected	5115	5277
Reflections with <i>I</i> > 2σ <i>I</i>	1777	2529
Number of parameters	361	468
Goodness of fit on <i>F</i> <sup>2</sup>	1.07	1.03
Final <i>R</i> indices [ <i>I</i> > 2σ <i>I</i> ]: <i>R</i> 1	0.0629	0.0867
<i>wR</i> 2	0.1743	0.2355
Max, min height in difference electron density map/e Å <sup>-3</sup>	0.243, -0.256	0.457, -0.322

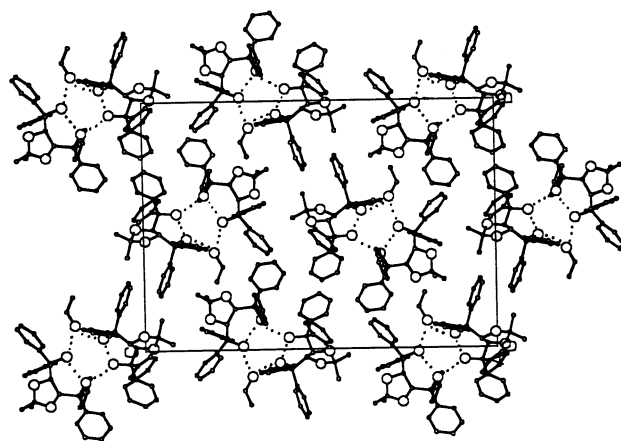
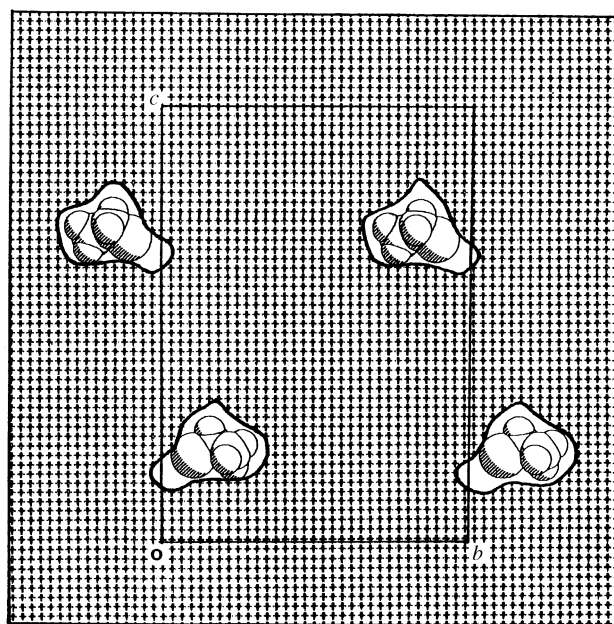
**Table 2** Details of hydrogen bonding distances

Atom labels	1 O...O (Å)	2 O...O (Å)
O(1A)···O(2A)	2.63(1)	2.60(1)
O(1A)···O(1C)	2.66(1)	2.66(1)
O(2A)···O(2B)	2.691(9)	2.721(9)
O(1B)···O(2B)	2.58(2)	2.57(1)
O(1B)···O(1C)	2.67(1)	2.68(1)

**Fig. 1** ORTEP plot of the asymmetric unit of **2** showing the atomic labelling scheme used (atoms are drawn at the 30% probability level)

asymmetric unit (shown in Fig. 1 for **2**) consists of two host molecules and one guest which are hydrogen bonded into a 10-membered ring. Details of the hydrogen bonding distances are given in Table 2. This hydrogen bonding motif is identical to that seen in the inclusion compounds of similar hosts with simple alkylamines.<sup>5</sup> It is also closely related to the hydrogen bonding motif observed in the structure of the uncomplexed host, **H**.<sup>5</sup> There, the molecules form dimers; each hydroxy acts as both proton donor and acceptor, forming an eight-membered hydrogen bonded ring system. In the inclusion compounds, the hydrogen bonded clusters are packed so that phenyl groups on adjacent rings form a hydrophobic region. This packing is illustrated in Fig. 2.

Analysis of the regions of the unit cell occupied by the host

**Fig. 2** Packing diagram of **2** viewed along [100]. Carbons are shown as filled circles and oxygens as open circles. Hydrogens have been omitted for clarity.**Fig. 3** Section through the unit cell at (3/4, *y*, *z*), illustrating the cavities in which guest molecules are situated. The region of the unit cell occupied by host molecules is shaded. Ethanol is drawn with van der Waals radii.

molecules indicated that the guest alcohols are located in cavities, as shown in Fig. 3.

#### Thermal analysis and kinetics of desolvation

The thermal analysis results are shown in Fig. 4. In each case, the guest loss reaction occurs in a single step with an onset temperature of 135 °C for **1** and 131 °C for **2**. This is significantly above the normal boiling points of methanol and ethanol, which indicates the stability of these compounds. The second endotherm in each DSC is caused by the melting of the host at 196 °C. Thermogravimetry confirmed the 2:1 stoichiometry modelled in the crystal structures, with mass losses of 3.1 and 4.3% observed for **1** and **2** respectively, which compare well with their expected mass losses of 3.3 and 4.7%.

A series of mass loss *vs.* time curves were obtained for the isothermal desorption of compounds **1** and **2**. An example of an *α* (extent of reaction) *vs.* time curve is shown in Fig. 5, and it is clearly deceleratory. A number of appropriate kinetic models were fitted to the data.<sup>9</sup> These consist of mechanisms based on either geometrical (contracting area, R2, contracting volume, R3) or diffusion (one, two or three dimensional) mechanisms. The model finally chosen was the Ginstling–Brounshtein mechanism (D4), which was the most linear fit over an *α* range of 0.1

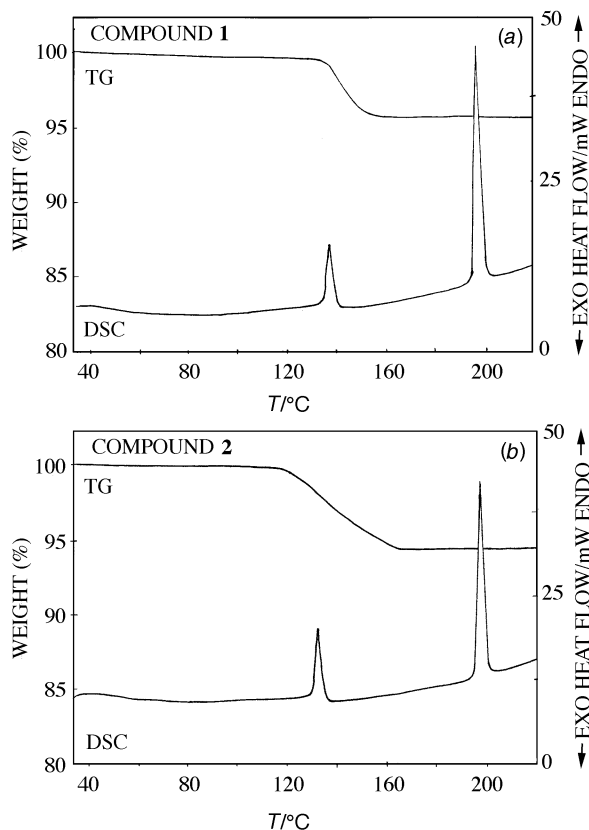


Fig. 4 TG and DSC curves for (a) **1** and (b) **2**

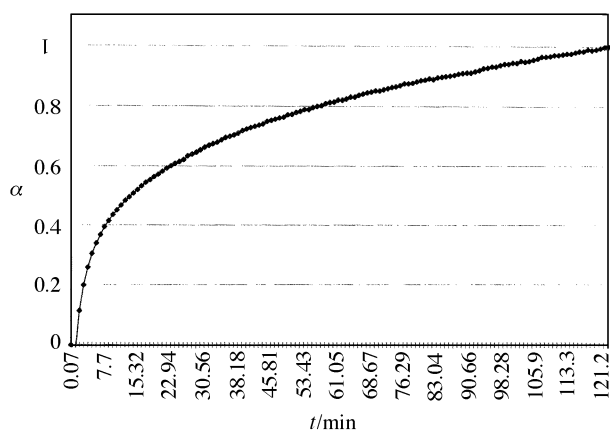


Fig. 5 An  $\alpha$  vs.  $t$  curve for **2** at 393 K

to 0.9, at all temperatures considered. The next closest model was the three dimensional diffusion mechanism (D3) which was, however, linear over a narrower  $\alpha$  range (0.1 to 0.75). The geometrical models were a considerably poorer fit. The semi-logarithmic plots of  $\ln k$  vs.  $1/T$  are shown in Fig. 6. Analysis of the slopes of these curves yielded activation energies of 170.0(1.2) for **1** and 178.7(1)  $\text{kJ mol}^{-1}$  for **2**.

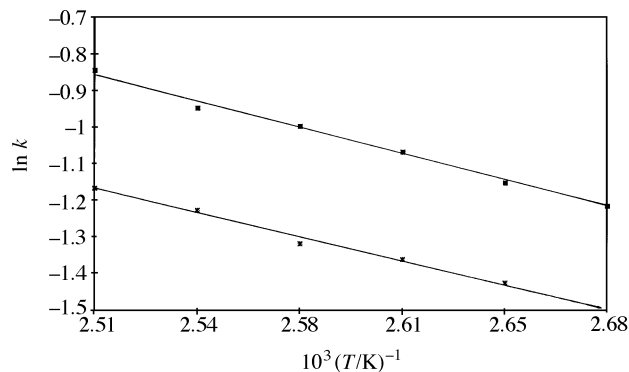


Fig. 6 Arrhenius plot for **1** (■) and **2** (×)

In diffusion limited reactions, the overall rate of reaction is determined by the movement of the reactant species to, or the products from, the reaction interface. As the desorption reaction proceeds, the barrier layer thickness increases, inhibiting diffusion of the product species away from the interface, and as a consequence, the reaction rate decelerates.

The D4 mechanism is a modification of a diffusion controlled mechanism in which the reactant front propagates towards the centre of the reacting particle in three dimensions, and in which allowance is made for the difference in the reactant and the product molar volumes.<sup>9</sup>

Thus the mechanism for desorption in **1** and **2** is the same, and the rate of this reaction is dependent on the rate of diffusion of the product away from the reaction interface. Similar values for the activation energy for this reaction were obtained for the two compounds, which is easily understood in light of their very similar crystal packing structures. We conclude therefore that this system is a poor model for attempts to separate these closely related alcohols.

## References

- 1 L. J. Barbour, M. R. Caira, A. Coetzee and L. R. Nassimbeni, *J. Chem. Soc., Perkin Trans. 2*, 1995, 1345.
- 2 M. R. Caira, A. Coetzee, L. R. Nassimbeni, E. Weber and A. Wierig, *J. Chem. Soc., Perkin Trans. 2*, 1995, 281.
- 3 M. R. Caira, L. R. Nassimbeni, N. Winder, E. Weber and A. Wierig, *Supramol. Chem.*, 1994, **4**, 135.
- 4 M. R. Caira, A. Coetzee, L. R. Nassimbeni and F. Toda, *J. Chem. Res. (S)*, 1996, 1565.
- 5 I. Goldberg, Z. Stein, E. Weber, N. Dörpinghaus and S. Franken, *J. Chem. Soc., Perkin Trans. 2*, 1990, 953.
- 6 G. M. Sheldrick, *Acta Crystallogr., Sect. A*, 1990, **46**, 467.
- 7 G. M. Sheldrick, *J. Appl. Crystallogr.*, unpublished results.
- 8 F. H. Allen, O. Kennard, D. G. Watson, L. Brammer, A. G. Orpen and R. Taylor, *J. Chem. Soc., Perkin Trans. 2*, 1987, S1.
- 9 M. E. Brown, *Introduction to Thermal Analysis—Techniques and Applications*, Chapman and Hall, London, New York and San Francisco, 1978.

Paper 6/05298C  
Received 29th July 1996  
Accepted 23rd October 1996